

The *MAP* Satellite Mission to Map the CMB Anisotropy

Lyman Page

Princeton University, Dept. of Physics, Jadwin Hall, Washington Rd

Abstract. The Microwave Anisotropy Probe (*MAP*) satellite is scheduled to launch in mid-2001. *MAP*'s goal is to produce a map of the anisotropy in the cosmic microwave background of unprecedented *accuracy* and precision. The guiding design principle has been the minimization of systematic effects. The instrument design and mapping strategy work in concert to take advantage of the unique opportunities afforded by deep space. We give an overview of the mission and compare the projected *MAP* error bars to recent measurements.

1. Introduction

The cosmic microwave background (CMB) is now widely recognized as one of the premier probes of cosmology. Other than foreground emission, which is subdominant and measurable, very little astrophysics stands between the observations and that which is of cosmological import (Tegmark et al. 2000). The theoretical framework is in place; the challenge before us is performing accurate and unassailable measurements of the properties of the CMB.

Since the discovery of the anisotropy by COBE/DMR (Smoot et al. 1992) experimental progress has been rapid. By the end of the last millennium, we knew that not only was there a peak in the angular spectrum, but we knew its amplitude, width, and position (Hu 2000, Dodelson & Knox 2000, Knox & Page 2000). The recent BOOMERanG (de Bernardis et al. 2000) and MAXIMA (Hanany et al. 2000) results have not only given us maps of the CMB but have impressively shown that peak in sharp relief. Analyses of the data (Bond et al. 2000, Jaffe et al. 2000) give us a glimpse of what may be learned from the primary anisotropy ($l < 2000$) in the context of adiabatic CDM models.

The future of CMB measurements is bright. In addition to results from many ground and balloon based experiments, the *MAP* satellite will map the CMB over the full sky to unprecedented accuracy and precision. *PLANCK* will follow later in the decade. The detection and characterization of the polarization will be crucial to verifying the picture unveiled by the temperature anisotropy and to placing further constraints on models. At $l > 2000$, the CMB can directly probe the formation of structures through the Ostriker-Vishniac effect, the Sunyaev-Zel'dovich effect, and lensing. Foreground emission at these scales will be more difficult to subtract from the data (Toffolatti et al. 1998) however.

2. MAP in comparison with other maps

The quest to make a large area map of the CMB anisotropy has been in cosmologists' minds for years. Early attempts (reviewed by Weiss 1980 and Partridge 1995) measured the CMB dipole, set limits on the anisotropy, and introduced mapping and analysis techniques. The goal was to produce a map with a temperature and error bar for each sky pixel. All of these experiments were done from balloons so that atmospheric fluctuations would not skew the map.

The modern era of CMB studies started with the 7° resolution full-sky COBE/DMR map (Smoot et al. 1992, Bennett et al. 1996) which unambiguously detected the anisotropy. This is still the map with the lowest systematic error; it is also the best checked map. One of the most important aspects of DMR is that pixel-to-pixel correlations are small, $\Sigma_{ij} = \sigma_i^2 \delta_{ij}$ (where Σ_{ij} is the covariance between pixels i and j) is an excellent approximation. Lineweaver et al. (1994) showed that for 60° lags, the DMR beam separation angle, the cross correlation was only 0.45% of the diagonal terms. In the final map, the S/N per beam resolution element was roughly two.

Next came FIRS (Meyer et al. 1991, Ganga et al. 1993) at 170 GHz and 3.8° resolution. For FIRS $\Sigma_{ij} \neq \sigma_i^2 \delta_{ij}$ but the off diagonal terms were small enough for the analyses. A spot check, requested by John Mather before the publication of Ganga et al. (1993), showed the largest to be of order 0.1 the diagonal elements. At the time, there was no way to handle the full covariance matrix for FIRS's 3500 pixels. The S/N per DMR beam was roughly $\sqrt{2}$.

QMAP (Devlin et al. 1999, Herbig et al. 1999, de Oliveira-Costa et al. 1999), with a resolution of 0.8° at 40 GHz, came after FIRS. Σ_{ij} was not diagonal for QMAP but the full covariance matrix was taken into account in the analysis. QMAP used the rotation around the NCP to achieve an interlocking scan strategy. The features one sees in QMAP are hot and cold spots in the CMB. The S/N is roughly 2 per beam over 530 square degrees.

Most recently, we have seen the very high S/N (> 5 per beam) BOOMERanG and MAXIMA results at $\approx 0.2^\circ$ resolution. Here too, the covariance matrix is not diagonal but has been taken into account. With their high resolution, one can clearly see the angular scale of an acoustic peak in the CMB. The analyzed BOOMERanG data covered 440 square degrees and MAXIMA covered 124 square degrees. Both experiments have more data which will be analyzed over the following few years.

As the sophistication in data analysis grows, more and more data sets are being presented as a "map" plus covariance matrix, so the distinction made above will be blurred. Indeed, maps are now commonly synthesized from interferometer data and scanning beam strategies. However, the ideal map is like DMR's: a set of temperatures and statistical weights, with ignorable off diagonal elements in the covariance matrix.

Producing a full-sky map with diagonal Σ_{ij} was one of MAP's design goals. The cornerstones of achieving this are 1) low $1/f$ noise in the instrument and detectors, and 2) a fully interlocking scan strategy¹. Concomitant with this goal

¹The notion of the interconnectedness of the scans was stressed in the proposal in 1995 but had to wait to be quantified by Wright (1996) and Tegmark (1997).

we aimed to ensure that orbit and spacecraft induced systematic errors would be negligible compared to the astrophysical signal.

3. Instrument description

MAP was proposed in June 1995, at the height of the “faster, better, cheaper” era; building began in June 1996. It was designed to be robust, thermally and mechanically stable, built of components with space heritage², and relatively easy to integrate and test.

Figure 1 shows a line drawing of the *MAP* satellite, though it could be a photograph. The satellite is completely built and put together. The long and demanding process of quality assessment is underway. As of this writing, *MAP* is well into its final observatory level environmental test program.

As a thumbnail sketch, the *MAP* instrument is comprised of ten symmetric, passively cooled, dual polarization, differential, microwave receivers. There are four receivers in W-band (94 GHz), two in V-band (61 GHz), two in Q-band (41 GHz), one in Ka band (33 GHz), and one in K band (23 GHz). The receivers are fed by back-to-back Gregorian telescopes. A more detailed description follows and more information may be obtained from <http://map.gsfc.nasa.gov/>.

In Figure 1, the large circular structure at the bottom is comprised of solar panels and flexible aluminized mylar/kapton insulation. It shields the instrument from thermal emission the Sun, Earth, and Moon. At launch, this is folded up so that the S/C can fit into the rocket fairing, though it deploys roughly 90 minutes after liftoff.

A hexagonal structure, “hex hub,” above the solar panel array holds the power supplies, instrument electronics, and attitude control systems. A one meter diameter thermally insulating gamma alumina cylinder (GAC) separates the hex hub and the instrument. The GAC supports a 190 K thermal gradient.

Two large (5.6 m² net) and symmetric radiators passively cool the input optics and front-end microwave electronics to less than 100 K. One can just make out the heat straps that connect the base of the radiators to the microwave components housed below the primary reflectors. There are no cryogenics or mechanical refrigerators.

3.1. Optics

The optics comprise two back-to-back shaped Gregorian telescopes. The primary mirrors are 1.4 by 1.6 m. The secondaries are roughly a meter across though most of the surface simply acts as a shield to prevent the feeds from directly viewing the Galaxy. The telescopes illuminate ten scalar feeds on each side, a few of which are visible in the figure. The primary optical axes are separated by 141° to allow differential measurements over large angles on a fast time scale. The feed centers occupy a 18 by 20 cm region in the focal plane, corresponding to a 4° by 4.5° array on the sky.

²Other than the HEMT amplifiers, which were custom designed, all components were “off-the-shelf.” I think it was a surprise to those of us not familiar with the satellite business how much testing was required of, and how many problems there were with, off-the-shelf hardware.

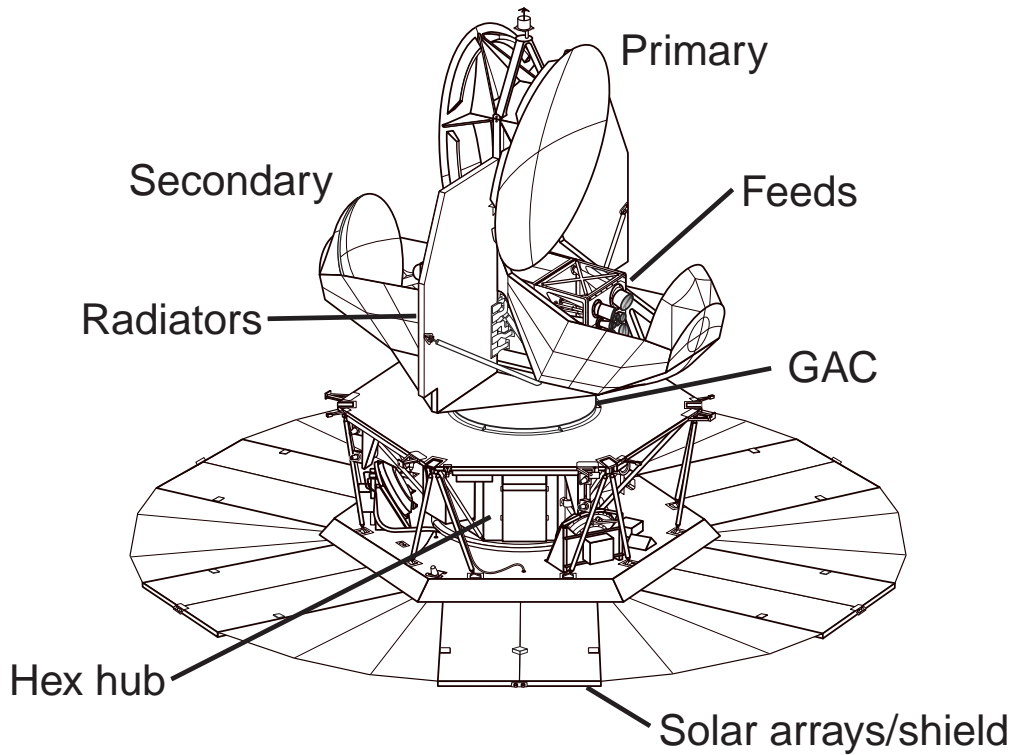


Figure 1. Outline of the *MAP* satellite. The overall height is 3.6 m, the mass is 830 kg, and the diameter of the large disk on the bottom is 5.1 m. Six solar arrays on the bottom of this disk supply the 400 Watts to power the spacecraft and instrument. Thermal blanketing between the hex hub and GAC, and between the GAC and radiators, shield the instrument from thermal radiation from the support electronics and attitude control systems. *MAP* will be launched in mid-2001 by a Delta 7425-10 from Kennedy Space Center. The mission life is 27 months.

At the base of each feed is an orthomode transducer (OMT) that sends the two polarizations supported by the feed to separate receiver chains. The microwave plumbing is such that a single receiver chain (half of a “differencing assembly”) differences electric fields with two nearly parallel linear polarization vectors, one from each telescope.

Precise knowledge of the beams is essential for accurately computing the CMB angular spectrum and for calibration. Because of the large focal plane the beams are not symmetric, as shown in Table 1. Cool down distortions of the optics will alter the W-band beams with respect to the ground based measurements so we give only an upper bound at this time. All beam profiles will be mapped in flight with Jupiter and other celestial sources.

Table 1. Approximate Instrument Characteristics by Frequency Bands

Band	f_{center} (GHz)	Δf_{noise} (GHz)	T_{HEMT} (K)	N_{chan}	θ_{FWHM} (deg)
K	23	5	25	2	0.75° by 0.95°
Ka	33	7	35	2	0.6° by 0.7°
Q	41	8	50	4	0.45° by 0.5°
V	61	11	80	4	0.3° by 0.35°
W	94	18	100	8	$< 0.23^\circ$

One of the design constraints was to minimize stray radiation from the Galaxy, Sun, and Earth. We use physical optics codes to compute the sidelobe pattern over the full sky as well as to compute the current distributions on the optics. We have also built a specialized test range to make sure that, by measurement, we can eliminate the Sun as a source of signal at $< 1 \mu\text{K}$ level in all bands. This requires knowing beam profiles down to roughly -45 dBi (gain above isotropic) or -105 dB from the W-band peak. We find that over much of the sky, the measured profiles differ from the predictions at the -50 dB level due to scattering off the feed horns and the structure that holds them.

We use a combination of the models and measurements to place a limit on the Galactic pickup in the sidelobes. At 90 GHz, less than $2 \mu\text{K}$ of Galactic signal should contaminate the boresite signal for observations with $|b| > 15^\circ$, before any modeling. As this adds in quadrature to the CMB signal, the affect on the angular spectrum will be negligible. The characterization of the sidelobes has been done by Chris Barnes.

3.2. Receivers

MAP uses “pseudo-correlation” receivers (Jarosik 2000) to measure the difference in power coming from the outputs of the OMTs at the base of the feeds, as shown in Figure 2. We use the term “pseudo” to refer to the fact that these radiometers use two hybrid tees and two square law detectors in place of the multiplier in a true correlation receiver. The “correlation” refers to the feature that the system is primarily sensitive to the correlated signal in the two arms.

The MAP mission was made possible by the HEMT-based amplifiers developed by Marian Pospieszalski (1992) at NRAO. These amplifiers achieve noise

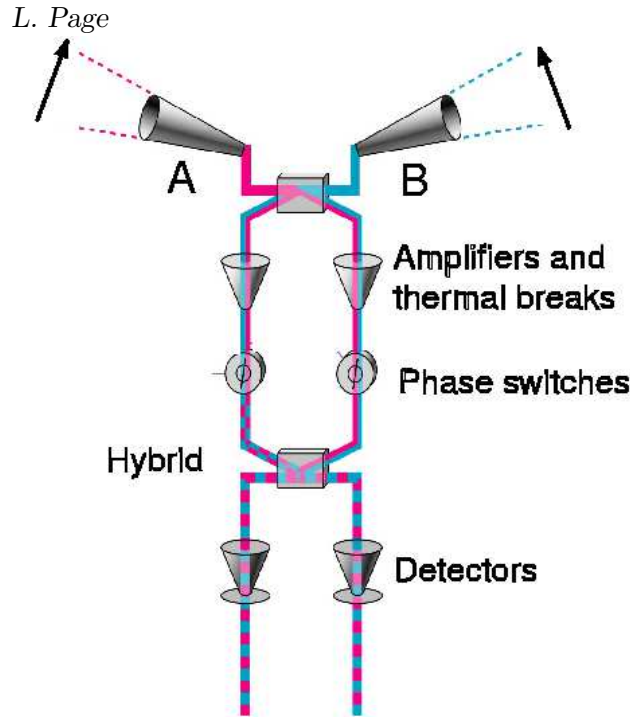


Figure 2. One half of a differencing assembly for detecting one polarization component. Hybrids (“magic tees”) split the inputs into two arms where the signal is amplified before recombining. There are actually two stages of amplification. The microwave filters between the lower hybrid and the detectors are not shown.

temperatures of 25-100 K at 80 K physical temperature (Pospieszalski & Wollock 2000). Of equal importance is that the amplifiers can be phase matched over a 20% fractional bandwidth, as is required by the receiver design.

In Figure 2, radiation from the two feeds is combined by a hybrid into $(A + B)/\sqrt{2}$ and $(A - B)/\sqrt{2}$ signals, where A and B refer to the amplitudes of the electric fields from one linear polarization of each feed horn. In one arm of the receiver, both A and B signals are amplified first by cold (< 100 K) and then by warm (290 K) HEMT amplifiers. Noise power from the amplifiers, which far exceeds the input power, is added to each signal by the first amplifiers. Ignoring the phase switch for a moment, the two arms are then recombined in a second hybrid and both outputs of the hybrid are detected after a band defining filter. Thus for each differencing assembly, there are four detector outputs, two for each polarization. In a perfectly balanced system, one detector continuously measures the power in the A signal plus the average radiometer noise while the other continuously measures the power in the B signal plus the average radiometer noise.

If the amplification factors for the fields are G_1 and G_2 for the two arms, the difference in detector outputs is $G_1 G_2 (A^2 - B^2)$. Note that the average power signal present in both detectors has cancelled so that small gain variations, which have a $1/f$ spectrum, act on the difference in powers from the two arms, which corresponds to less than 1 K, rather than on the total power which corresponds

to roughly 100 K in W-band. The system is stabilized further by toggling one of the phase switches at 2.5 kHz and coherently demodulating the detector outputs. (The phase switch in the other arm is required to preserve the phase match between arms and is jammed in one state.) The 2.5 kHz modulation places the desired signal at a frequency above the $1/f$ knee of the detectors and video amplifiers as well as rejecting any residual effects due to $1/f$ fluctuations in the gain of the HEMT amplifiers. The power output of each detector is averaged for between 51 and 128 ms and telemetered to the Earth. In total, there are forty signals (only half contain independent information) plus instrument housekeeping data resulting in a data rate of 110 MBy/day.

The power spectrum of the noise shows that it is effectively white between 0.008 Hz, the spin rate of the satellite, and 2.5 kHz. The autocorrelation function shows only a spike at zero lag and a 1.2% correlation between adjacent samples (in W-band) due to the antialiasing filter. All tests show that the noise is stationary and Gaussian for days at a time.

Although *MAP*'s differential design was driven by the $1/f$ noise in the amplifiers, it is also very effective at reducing the effects of $1/f$ thermal fluctuations of the spacecraft itself. The thermal stability of deep space combined with the insensitivity to the spacecraft's slow temperature variations should result in an extremely stable instrument. Outside of the antialiasing filter and finite sampling time, effects which are computable, measured, and non-random, we have not been able to identify other effects that will correlate one measurement to the next.

3.3. Scan strategy

The other key aspect of producing a map with $\Sigma_{ij} = \sigma_i^2 \delta_{ij}$, in addition to low system $1/f$, is a highly interlocking scan strategy. In any measurement, a baseline instrumental offset along with its associated drift, must be subtracted. Without cross hatched scans this subtraction can correlate pixels over large swaths, resulting in striped maps and substantially more involved analyses.

MAP observes from a low maintenance Lissajous orbit at L2, with the Sun Earth and Moon always behind, as shown in Figure 3. Corrections to the orbit are applied roughly once per season through thruster jets; there is only one mode of operation. *MAP* will be the first satellite to stay at L2 for an appreciable time.

MAP spins around its axis with a period of 2 min and precesses around a 22.5° degree cone every hour so that the beams follow a spirograph pattern. Consequently, $\approx 30\%$ of the sky is covered in one hour, before the instrument temperature can change appreciably. This motion is accomplished with three spinning momentum wheels; the net angular momentum of the satellite is near zero. The axis of this combined rotation/precession sweeps out approximately a great circle as the Earth orbits the sun. In six months, the whole sky is mapped. Systematic effects at the spin period of the satellite are the most difficult to separate from true sky signal. Such effects, driven by the Sun, are minimized because the instrument is always in the shadow of the solar array and the precession axis is fixed with respect to the Earth-Sun line.

The combination of *MAP*'s four observing time scales (2.5 kHz, 2.1 min, 1 hour, 6 months) and the heavily interlocked pattern result is a strong spatio-

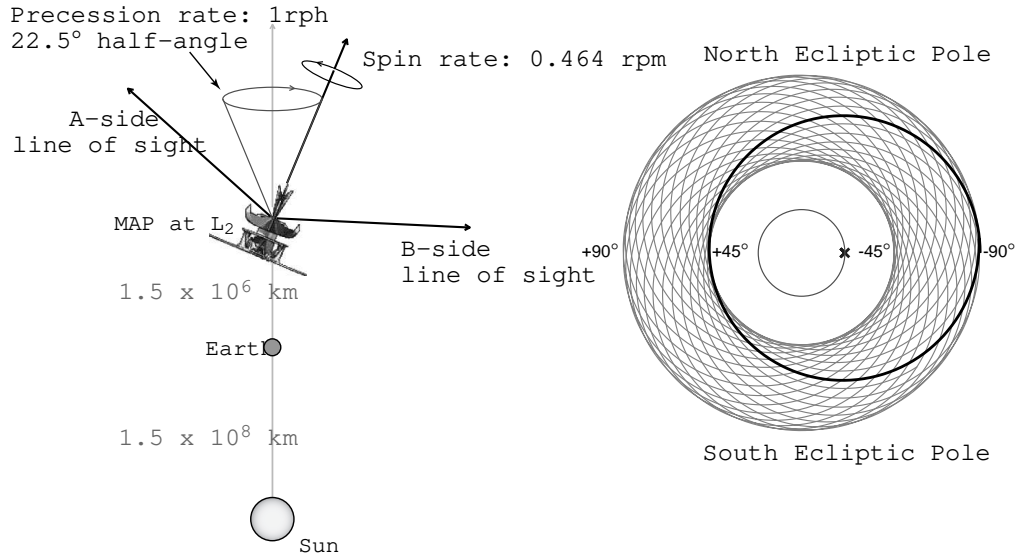


Figure 3. *MAP*'s scan pattern from L2. The dark circle on the left-hand drawing depicts the path covered by two beams for one rotation, the innermost circle is the path of the spin axis during one precession.

temporal filter for any signal fixed in the sky. A pipeline for simulating the mission, the amplifier characteristics, the beam profiles, and producing maps from the time ordered data is written. Using the measured amplifier characteristics, we can form the two point function of a simulated noise map. It shows that the pixel-pixel correlations are negligible with the exception of a $< 1\%$ nearest neighbor correlation from the antialiasing filter and a $\sim 0.1\%$ correlation at angles of the beam separation. See Hinshaw (2000) for more details.

3.4. Science from *MAP*

We emphasize again that the primary goal of MAP is to produce high fidelity polarization-sensitive full-sky multi-frequency maps of the microwave sky. With such maps we can not only determine the anisotropy in the CMB but we can test our fundamental assumptions about the cosmos. For instance, perhaps the best fit model is not a simple adiabatic CDM variant but has some isocurvature modes mixed in.

If the CMB temperature fluctuations are Gaussian with random phases, as the current data suggest, then the cosmological information may be obtained from the angular spectrum. An example is shown in Figure 4. The limit to which we can know the angular spectrum is set by the number of independent patches of sky corresponding to a given angular scale, or equivalently the number parameters needed to describe a mode. For instance, five parameters determine the quadrupole. No matter how well we measure these, we cannot know the fractional variance of the parent distribution better than $\sqrt{2/(2l+1)} = 0.63$. This is the ‘‘cosmic variance’’ limit and is one of the motivations for a full-sky map. *MAP* will be cosmic variance limited up to $l \approx 500$ in W-band. In

other words, in principle it is not possible to determine the angular spectrum better than this. More information may be obtained from high S/N polarization measurements however.

One of the largest uncertainties of existing measurements is the calibration. Limitations come from not knowing the beam profiles precisely and from the intrinsic uncertainty in the calibration sources. The flux from planets is known to $\approx 5\%$ depending on frequency. Although the dipole has been used to calibrate a number of mapping experiments (Meyer et al. 1991, de Bernardis et al. 2000, Hanany et al. 2000), it is difficult to measure with limited sky coverage because of its covariance with typical scan patterns. *MAP* like DMR, will calibrate using the change in the dipole caused by the Earth's motion around the Sun. The calibration error will be $< 1\%$.

In Figure 4, we compare the projected *MAP* uncertainties with the state-of-the-art. We have included calibration error in both plots. The right hand plot shows the amplitude and position of the first peak ($50 < l < 420$) based on Knox & Page (2000). This is a relatively *cosmological model independent* parametrization of the peak. It differs from the work of Bond and colleagues (see these proceedings) in that a CDM variant is not assumed and there is no marginalization over nonrelevant parameters, consequently the error bars are smaller. Though one should not put too much stock in interpreting the contours beyond the $\approx 2\sigma$ level, the plot shows that, despite high precision, we are still not in complete agreement on the position and amplitude of the first peak.

There will be much more to do with the *MAP* data than fit cosmological models. A partial list includes understanding Galactic foreground emission (is there spinning dust?) and extragalactic sources (they are separated from the CMB through their frequency spectrum and positive definiteness), a search for time variable sources, a search for non-standard topologies, a measurement of the polarization-temperature cross correlation, a search for the large scale Sunyaev-Zel'dovich effect, a measurement of the cross-correlation with the Solan Digital Sky Survey to assess structure formation at lower redshift ($z < 1000$).

Over the next two years, our current picture of the primary anisotropy will become clearer as more BOOMERanG and MAXIMA data are analyzed and as new data come in from ACBAR, Arkeops, BEAST, CBI, DASI, MINT, TopHat, VSA, and others. The full data set will of course be interesting on its own, and will be essential for ensuring that the picture we get from *MAP* extrapolates as predicted in both frequency and angular scale. The next generation of polarization measurements of the primary anisotropy will take us beyond *MAP*'s polarization sensitivity and add a new dimension to CMB studies. It will not be too long before CMB experiments will be calibrated on the primary anisotropy, a prospect difficult to believe just a few years ago.

Acknowledgments. The work on which this article is based, except for the righthand panel in Figure 4, was done by the *MAP* science team³ and the *MAP* satellite project led by Liz Citrin (Project Manager) and Cliff Jackson (Systems

³Chuck Bennett (NASA/GSFC, PI), Mark Halpern (UBC), Gary Hinshaw (NASA/GSFC), Norm Jarosik (Princeton), Al Kogut (NASA/GSFC), Michele Limon (Princeton), Stephan Meyer (Chicago), Lyman Page (Princeton), David Spergel (Princeton), Greg Tucker (Brown), David Wilkinson (Princeton), Ed Wollack (NASA/GSFC), and Ned Wright (UCLA).

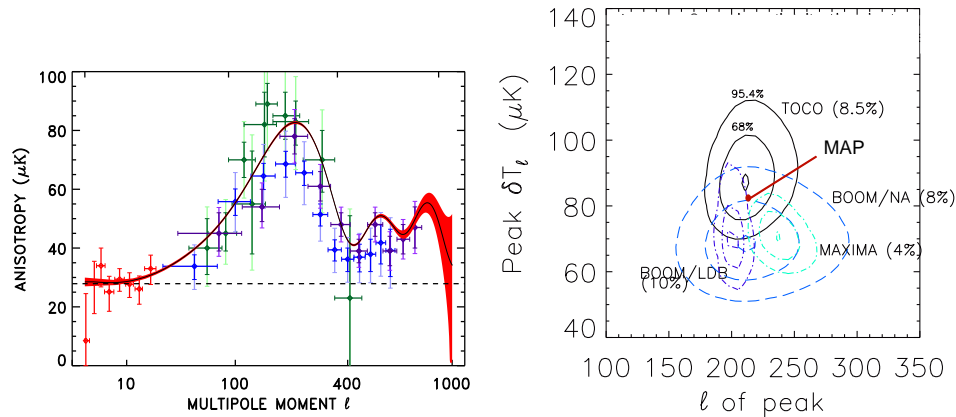


Figure 4. *Left.* The projected *MAP* error bars for a band averaging of $\Delta\ell = 50$ superimposed on a popular model along with the BOOMERanG, MAXIMA, and TOCO (Torbet et al. 1999, Miller et al. 1999) data. The calibration uncertainty is indicated by the light lines behind the thick lines. It is not usually plotted like this because the calibration is common to all data in a set. *Right.* An analysis of the peak following the Knox & Page (2000) Gaussian/Temperature method. Calibration error is included and shown in parentheses. The BOOMERanG N/A data are from Mauskopf et al. (2000). The small solid dot shows the projected *MAP* error.

Engineer) at NASA/GSFC. Over a hundred NASA employees and contractors have dedicated themselves to making *MAP* work.

References

- Bennett C. L. et al. 1996, ApJ, 464, L1
 Bond, J. R. et al. 2000, These proceedings and astro-ph/0011381 and astro-ph/0011379
 de Bernardis, P. et al. 2000, Nature, 404, 955
 de Oliveira-Costa, A. et al. 1998, ApJ, 509, L77
 Devlin, M. J. et al. 1998, ApJ, 509, L69
 Dodelson, S. & Knox, L. 2000, Phys.Rev.Lett, 84, 3523
 Ganga, K. et al. 1993, ApJ, 410, L57
 Hanany, S. et al. 2000, astro-ph/0005123
 Herbig, T. et al. 1998, ApJ, 509, L73
 Hinshaw, G. 2000, astro-ph/0011555
 Hu, W. 2000, astro-ph/0002520
 Jaffe, A. et al. 2000, astro-ph/0007333
 Jarosik, N. 2000, "The Use of Cryogenic HEMT Amplifiers in Wide Band Radiometers." Proceedings of the European Gallium Arsenide Application Symposium, Paris, France (GAAS2000)

- Knox, L. & Page, L. 2000, *Phys.Rev.Lett*, 85, 1366
- Lineweaver, C. et al. 1994, *ApJ*, 436, 452
- Mauskopf, P. 2000, *ApJ*, 536, L59
- Meyer, S. S., Cheng, E. S., & Page, L. A. 1991, *ApJ*, 371, L7
- Miller, A. D. et al. 1999, *ApJ*, 524, L1
- Partridge, B. 1995, *3K: The Cosmic Microwave Background Radiation*, Cambridge University Press, New York
- Pospieszalski, M. W. 1992, *Proc. IEEE Microwave Theory Tech.*, MTT-3, 1369
and Pospieszalski, M. W. et al. 1994, *Proc. IEEE Microwave Theory Tech.*, MTT-3, 1345
- Pospieszalski, M. W. & Wollack, E. 2000, "Ultra-Low-Noise, InP Field Effect Transistors Amplifiers for Radio Astronomy Receivers," *Proceedings of the European Gallium Arsenide Application Symposium, Paris, France (GAAS2000)*
- Smoot, G. et al. 1992, *ApJ*, 153, L1
- Tegmark, M. 1997, *Phys.Rev.D*, 56
- Tegmark, M. et al. 2000, *ApJ*, 530, 133
- Toffolatti, L. et al. 1998, *MNRAS*, 297, 117
- Torbet, E. et al. 1999, *ApJ*, 521, L79
- Wright, E. L. 1996, *astro-ph/9612006*
- Weiss, R. 1980, *ARA&A*, 18, 489-535